

Synthesis, Structure, and Thermochemistry of the Formation of the Metal–Metal Bonded Dimers $[\text{Mo}(\mu\text{-TeAr})(\text{CO})_3(\text{P}^i\text{Pr}_3)]_2$ (Ar = Phenyl, Naphthyl) by Phosphine Elimination from $^*\text{Mo}(\text{TePh})(\text{CO})_3(\text{P}^i\text{Pr}_3)_2$

John J. Weir, James E. McDonough, George Fortman, Derek Isrow, Carl D. Hoff,* Brian Scott, and Gregory J. Kubas*

Department of Chemistry, University of Miami, Coral Gables, Florida 33124, and Structural Inorganic Chemistry Group, Chemistry Division, MS J514, Los Alamos National Laboratory, Los Alamos, New Mexico 87545

Received August 31, 2006

The complexes $(^*\text{TeAr})\text{Mo}(\text{CO})_3(\text{P}^i\text{Pr}_3)_2$ (Ar = phenyl, naphthyl; ^iPr = isopropyl) slowly eliminate P^iPr_3 at room temperature in a toluene solution to quantitatively form the dinuclear complexes $[\text{Mo}(\mu\text{-TeAr})(\text{CO})_3(\text{P}^i\text{Pr}_3)]_2$. The crystal structure of $[\text{Mo}(\mu\text{-Te-naphthyl})(\text{CO})_3(\text{P}^i\text{Pr}_3)]_2$ is reported and has a Mo–Mo distance of 3.2130 Å. The enthalpy of dimerization has been measured and is used to estimate a Mo–Mo bond strength on the order of 30 kcal mol⁻¹. Kinetic studies show the rate of formation of the dimeric chalcogen bridged complex is best fit by a rate law first order in $(^*\text{TeAr})\text{Mo}(\text{CO})_3(\text{P}^i\text{Pr}_3)_2$ and inhibited by added P^iPr_3 . The reaction is proposed to occur by initial dissociation of a phosphine ligand and not by radical recombination of 2 mol of $(^*\text{TeAr})\text{Mo}(\text{CO})_3(\text{P}^i\text{Pr}_3)_2$. Reaction of $(^*\text{TePh})\text{Mo}(\text{CO})_3(\text{P}^i\text{Pr}_3)_2$, with L = pyridine (py) or CO, is rapid and quantitative at room temperature to form PhTeTePh and $\text{Mo}(\text{L})(\text{CO})_3(\text{P}^i\text{Pr}_3)_2$, in keeping with thermochemical predictions. The rate of reaction of $(^*\text{TeAr})\text{W}(\text{CO})_3(\text{P}^i\text{Pr}_3)_2$ and CO is first-order in the metal complex and is proposed to proceed by the associative formation of the 19 e⁻ radical complex $(^*\text{TePh})\text{W}(\text{CO})_4(\text{P}^i\text{Pr}_3)_2$ which extrudes a $^*\text{TePh}$ radical.

Introduction

Oxidative-addition/reductive-elimination equilibria are influenced strongly by the role of ancillary ligands. This is well-documented for molecular hydrogen compounds, where replacement of a weak σ donor such as carbon monoxide by a more basic phosphine ligand can have a dramatic influence on whether H_2 forms a molecular hydrogen complex, undergoes oxidative addition to form a dihydride, or establishes a tautomeric equilibrium of both. In addition, examples of both σ bond coordination and oxidative addition are known for C–H, Si–H, and C–X bonds. There are relatively few cases, except for dihydrogen itself, in which the free energies of the two products are closely enough matched that both tautomers can be observed simultaneously in solution.¹

The oxidative-addition/reductive-elimination of RE–ER (E = S, Se, Te) is an important reaction in metal/chalco-

genide chemistry.² Several potential coordination modes for bonding are available. For mononuclear complexes, as shown in Scheme 1, the predominant modes of binding are either as a coordinate complex through the lone pair on E (**1A**) or as an oxidative addition product (**1D**).

A reasonable explanation for that is that lone-pair coordination is stronger than bonded-pair coordination. The distinction between a σ -bond donor (**1B**) and a chelating bis-E lone-pair donor complex (**1C**) cannot be made on the basis of structural studies alone; however, there are relatively few such structures known.³

The redox chemistry of dinuclear complexes is more complex, and representative structures for $[\text{L}_n\text{M}]_2[\text{RE-ER}]$ complexes are shown in Scheme 2. End on structures in

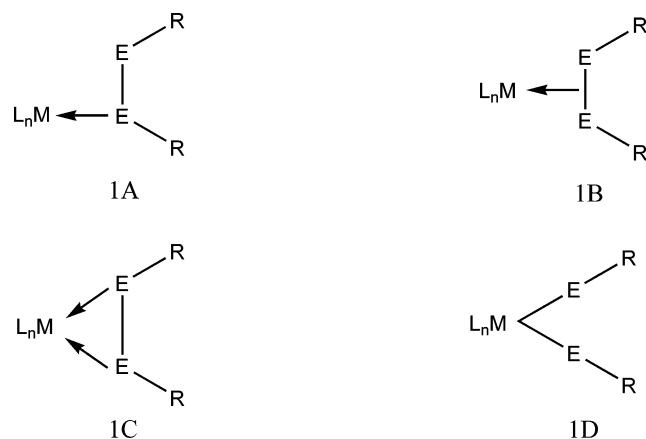
* To whom correspondence should be addressed. E-mail: c.hoff@miami.edu (C.D.H.), kubas@lanl.gov (G.J.K.).

(1) Kubas, G. J. *Metal-Dihydrogen and σ -Bond Complexes*; Kluwer Academic/Plenum Publishers: New York, 2001.

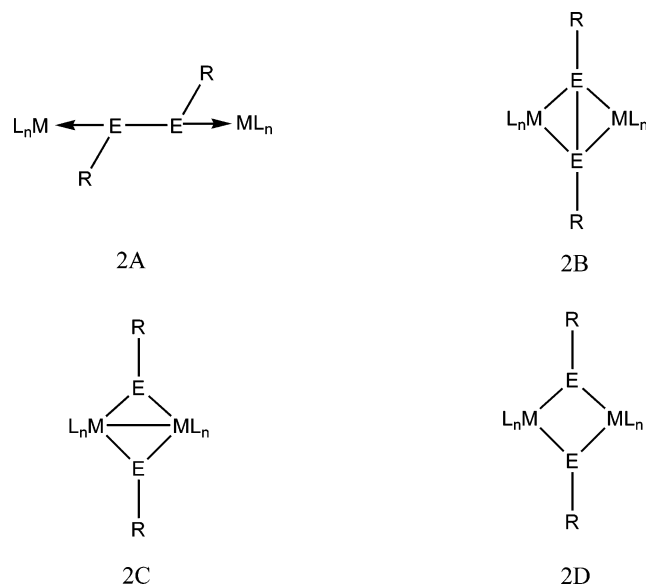
(2) *Transition Metal Sulfur Chemistry*; Stiefel, E. I., Matsumoto, K., Eds.; ACS Symposium Series 653; American Chemical Society: Washington, DC, 1996.

(3) A search of the Cambridge database yielded only five structures corresponding to structure **1C**. A typical one is the $\text{NbCl}_4(\text{S}_2\text{Me}_2)$ cation which retains a S–S bond and in which the methyl disulfides are symmetrically bound. (McKarns, P. J.; Heeg, M. J.; Winter, C. H. *Inorg. Chem.* **1998**, *37*, 4743.) The high oxidation state of Nb(V) presumably rules out oxidative addition.

Scheme 1



Scheme 2

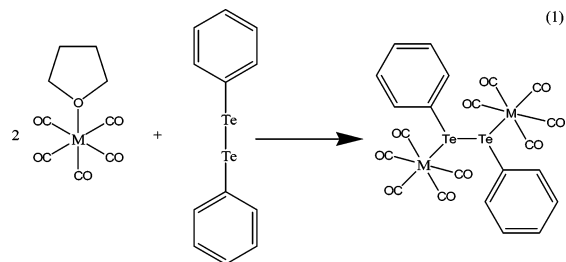


which the RE–ER bond is retained, as shown in structure **2A** of Scheme 2, are relatively rare. Furthermore, the authors could find no examples of bridging structures in which the RE–ER bond is retained in dinuclear complexes, such as that depicted in **2B**.⁴ In spite of the fact that characterized structures such as that shown in **2A** and **2B** are rare, they are logical intermediates in the formation of the more common bridging alkyl or aryl chalcogenide complexes which may contain a metal–metal bond (**2C**) or be held together only by bridging μ -ER ligands (**2D**).

An additional oxidative-addition/reductive-elimination reaction channel in complexes of structure **2A** is homolytic cleavage of the RE–ER bond present to yield monomeric radicals. For the unsubstituted pentacarbonyl complexes shown in eq 1 of Cr, Mo, and W, the type **2A** structure is

(4) Search of the Cambridge database yielded no structures in which a disulfide (RS–SR) bridges two metals with an intact S–S bond as in **2B**. Structures in which the S–S unit with no R groups attached bridges two metals are more widely known. See, for example, Helton, M. E.; Chen, P.; Paul, P. P.; Tyeklar, Z.; Sommer, R. D.; Zakharov, L. N.; Rheingold, A. L.; Solomon, E. I.; Karlin, K. D. *J. Am. Chem. Soc.* **2003**, *125*, 1160. The possibility of chalcogen–chalcogen bonds in edge-sharing square planar d^8 complexes was recently investigated theoretically: Aullon, G.; Hamidi, M.; Lledos, A.; Alvarez, S. *Inorg. Chem.* **2004**, *43*, 3702.

stable, and cleavage of the PhTe–TePh is not reported to occur at room temperature.



The Te–Te bond⁵ in $[\mu\text{-PhTe-TePh}][\text{Mo}(\text{CO})_5]_2$ of 2.803 Å, however, is longer than that in uncomplexed PhTe–TePh of 2.712 Å⁶ and possibly indicative of some Te–Te bond weakening but short of oxidative addition.

In contrast, the reaction of PhE–EPh (E = S, Se, Te) with the phosphine substituted complexes $\text{M}(\text{CO})_3(\text{P}^i\text{Pr}_3)_2$ (M = Mo, W) was proposed to proceed via formation of an intermediate complex $[\mu\text{-PhE-EPh}][\text{M}(\text{CO})_3(\text{P}^i\text{Pr}_3)_2]_2$ which subsequently underwent homolytic fission of the PhE–EPh bond to yield stable free radicals.⁷ During calorimetric studies of the $(^*\text{TePh})\text{Mo}(\text{CO})_3(\text{P}^i\text{Pr}_3)_2$ complex, however, it was discovered that this complex slowly reacts to form a bridging dinuclear complex. A plausible mechanism for the formation of such a dinuclear complex would be that shown in Figure 1.

The mechanism in Figure 1 involves initial radical recombination to form a complex of type **2A**. Following that, it is similar to one proposed earlier⁵ for the known conversion of $[\mu\text{-PhTe-TePh}][\text{M}(\text{CO})_5]_2$ to $[\text{Mo}(\text{CO})_4(\mu\text{-TePh})]_2$.⁸ The key steps in the mechanism are the loss of phosphine ligands to form a structure of type **2B** in which the PhTe–TePh bond is retained followed by rearrangement to a structure of type **2C** in which the final metal–metal bonded product is formed. This paper reports structural, thermochemical, and kinetic studies which were begun with the goal of proving (or disproving) a mechanism of formation of $[\text{Mo}(\mu\text{-TeAr})(\text{CO})_3(\text{P}^i\text{Pr}_3)]_2$ (Ar = phenyl, naphthyl) from $(^*\text{TePh})\text{Mo}(\text{CO})_3(\text{P}^i\text{Pr}_3)_2$ similar to that in Figure 1.

Experimental Section

General Considerations. All operations were performed in a Vacuum Atmospheres drybox under an atmosphere of purified argon or utilizing standard Schlenk tube techniques under argon.

- (5) (a) Pasynskii, A. A.; Torubaer, Y. V.; Lyakina, A. Y.; Drukovskii, A. G.; Lyalikov, V. G.; Skabitskii, I. V.; Lysenko, K. A.; Nefedov, S. E. *Russ. J. Coord. Chem.* **1998**, *24*, 745. (b) Pasynskii, A. A.; Torubaer, Y. V.; Drukovskii, A. V.; Eremenko, I. L.; Vegini, D.; Nefedov, S. E.; Dobrokhotova, A. V.; Yanovskii, A. I.; Struchkov, Y. T. *Russ. J. Inorg. Chem.* **1997**, *42*, 36. (c) Pasynskii, A. A.; Torubaer, Y. V.; Drukovskii, A. V.; Eremenko, I. L.; Vegini, D.; Nefedov, S. E.; Dobrokhotova, A. V.; Yanovskii, A. I.; Struchkov, Y. T. *Russ. J. Inorg. Chem.* **1997**, *42*, 957. (d) Pasynskii, A. A.; Torubaer, Y. V.; Drukovskii, A. V.; Eremenko, I. L.; Vegini, D.; Nefedov, S. E.; Dobrokhotova, A. V.; Yanovskii, A. I.; Struchkov, Y. T. *Russ. J. Inorg. Chem.* **1996**, *41*, 2006.
- (6) Llabres, P. G.; Dupont, O. D. *Acta Crystallogr., Sect. B* **1972**, *28*, 2438.
- (7) McDonough, J. E.; Weir, J. J.; Sukcharoenphon, K.; Hoff, C. D.; Kryatov, O. P.; Rybak-Akimova, E. V.; Scott, B.; Kubas, G. J.; Stephens, F. H.; Mendriatta, A.; Cummins, C. C. *J. Am. Chem. Soc.* **2006**, *128*, 10295.
- (8) Vogt, T.; Strahle, J. Z. *Naturforsch.* **1985**, *40B*, 1599.

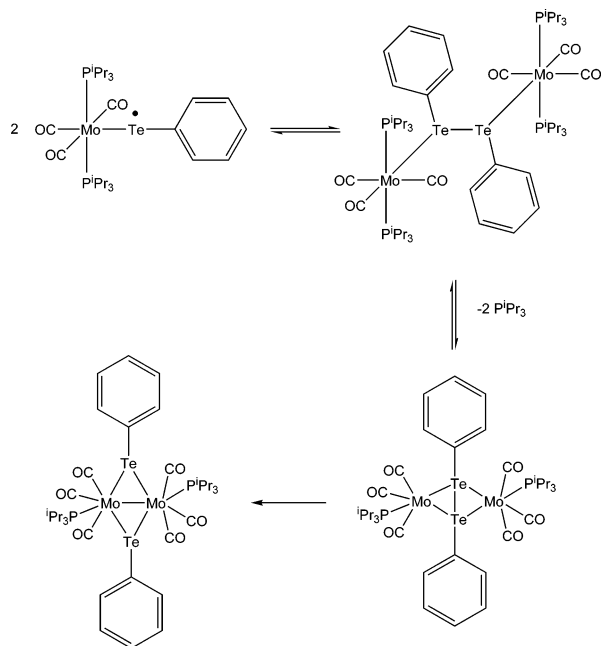


Figure 1. Plausible mechanism for formation of $[\mu\text{-PhE-EPH}][\text{M}(\text{CO})_3(\text{P}^i\text{Pr}_3)_2]_2$ from $(^*\text{TePh})\text{Mo}(\text{CO})_3(\text{P}^i\text{Pr}_3)_2$.

Toluene and heptane were purified by distillation under argon from sodium benzophenone ketyl into flame-dried glassware. Methylene chloride was refluxed under an argon atmosphere over P_2O_5 and then distilled. Pyridine was distilled from BaO under argon atmosphere. Fourier transform infrared (FTIR) data were obtained on a Perkin-Elmer 2000 spectrometer/microscope system. Solution calorimetric data were obtained using a Setaram C-80 Calvet calorimeter. NMR spectra were obtained on a Bruker AVANCE 400 MHz spectrometer. Mass spectra (MS) were obtained on a VG MASSLAB TRIO-2 using fast atom bombardment (FAB) techniques. Phenyl ditelluride and naphthyl ditelluride were obtained from Aldrich Chemical and were recrystallized from methylene chloride/heptane mixtures by slow evaporation and cooling prior to use. Carbon monoxide was obtained from Matheson Gas and was of 99.9995% purity. Microanalysis was performed by Galbraith Laboratories, Knoxville, TN.

Synthesis of $[\text{Mo}(\mu\text{-TePh})(\text{CO})_3(\text{P}^i\text{Pr}_3)_2]_2$. In the glovebox, 2.025 g of solid $\text{Mo}(\text{CO})_3(\text{P}^i\text{Pr}_3)_2$ and 0.8177 g of PhTe-TePh were weighed into a 100 mL Schlenk tube. The flask was purged with argon, and 25 mL of distilled toluene was added. The solution immediately changed color from purple to the pine green color characteristic of $(^*\text{TePh})\text{Mo}(\text{CO})_3(\text{P}^i\text{Pr}_3)_2$. An initial FTIR spectrum confirmed quantitative conversion to the radical product with bands at 1973 and 1875 cm^{-1} . The solution was allowed to stand, and the color changed overnight to orange brown. A FTIR spectrum showed a quantitative conversion to $[\text{Mo}(\mu\text{-TePh})(\text{CO})_3(\text{P}^i\text{Pr}_3)_2]_2$ with bands at 2008, 1971, and 1900 cm^{-1} . A mass spectrum for $[\text{Mo}(\mu\text{-TePh})(\text{CO})_3(\text{P}^i\text{Pr}_3)_2]_2$ showed only a very weak parent peak at $P = 1089 \text{ cm}^{-1}$ but did show a strong peak at 1061 cm^{-1} assigned to P-CO and at 1033 cm^{-1} assigned to P-2CO as well as other fragmentation patterns in keeping with the proposed dimeric structure. A sample for elemental analysis was recrystallized by slow evaporation of a toluene/heptane solution. Anal. Calcd for $[\text{Mo}(\mu\text{-TePh})(\text{CO})_3(\text{P}^i\text{Pr}_3)_2]_2$: C, 39.66; H, 4.77; Mo, 17.6; Te, 23.4. Found: C, 39.87; H, 5.09; Mo, 16.8; Te, 21.8. In separate experiments, the liberation of P^iPr_3 , which was detected by its characteristic unpleasant odor, was confirmed by NMR spectroscopy, and the addition of (cycloheptatriene) $\text{Mo}(\text{CO})_3$ to the reaction solution and observing its conversion to $\text{Mo}(\text{CO})_3(\text{P}^i\text{Pr}_3)_2$ were

Table 1. Crystallographic Data for $[\text{Mo}(\mu\text{-Te-naphthyl})(\text{CO})_3(\text{P}^i\text{Pr}_3)_2]_2$

empirical formula	$\text{C}_{44}\text{H}_{56}\text{O}_6\text{P}_2\text{Mo}_2\text{Te}_2$	fw	1189.91
<i>a</i>	11.3864(3) Å	space group	$P\bar{1}$ (No. 2)
<i>b</i>	14.2809(3) Å	<i>T</i>	-132(1) °C
<i>c</i>	16.9416(4) Å	λ	0.710731 Å
α	103.4117(3) Å	D_{calcd}	1.509 g cm^{-3}
β	91.5691(3) Å	μ	16.70 cm^{-1}
γ	101.3573(3) Å	$R(F_o^2)^a$	0.0283
<i>V</i>	2619.5(1) Å ³	$R_w(F_o^2; I > 2\sigma)^a$	0.0833
<i>Z</i>	2		

^a $R = (\sigma|F_o| - |F_c|)/\sigma|F_o|$ and $R_w = [\sum[w(F_o^2 - F_c^2)^2]/\sum[w(F_o^2)^2]]^{1/2}$. The parameter $w = 1/[\sigma^2(F_o^2) + (0.0851P)^2]$.

confirmed by FTIR analysis. All attempts to grow crystals of $[\text{Mo}(\mu\text{-TePh})(\text{CO})_3(\text{P}^i\text{Pr}_3)_2]_2$ suitable for crystal structure determination failed.

Crystal Growth of $[\text{Mo}(\mu\text{-Te-naphthyl})(\text{CO})_3(\text{P}^i\text{Pr}_3)_2]_2$. Preparation of $[\text{Mo}(\mu\text{-Te-naphthyl})(\text{CO})_3(\text{P}^i\text{Pr}_3)_2]_2$ was performed in a method identical to that described above for $[\text{Mo}(\mu\text{-TePh})(\text{CO})_3(\text{P}^i\text{Pr}_3)_2]_2$. FTIR spectroscopic data for the complex showed bands at 2005, 1970, and 1906 cm^{-1} in a pattern similar to that for $[\text{Mo}(\mu\text{-TePh})(\text{CO})_3(\text{P}^i\text{Pr}_3)_2]_2$. Mass spectroscopic data for $[\text{Mo}(\mu\text{-Te-naphthyl})(\text{CO})_3(\text{P}^i\text{Pr}_3)_2]_2$, $P = 1191 \text{ cm}^{-1}$, showed a strong peak centered at 1163 cm^{-1} for P-CO. The sample was recrystallized once from toluene/heptane. The recrystallized material was dissolved in toluene, filtered into a crystallization tube, layered with heptane, and sealed under vacuum. The tube was placed in the freezer for several weeks. During that time, red-brown crystals were grown. The crystals were isolated in the glovebox for structural analysis.

Determination of Crystal Structure. The crystal was mounted in a nylon cryoloop from Paratone-N Oil under an argon gas flow. The data were collected on a Bruker SMART APEX II charge-coupled device (CCD) diffractometer, with a KRYO-FLEX liquid nitrogen vapor cooling device. The instrument was equipped with a graphite monochromatized Mo $K\alpha$ X-ray source ($\lambda = 0.71073 \text{ \AA}$) with MonoCap X-ray source optics. A hemisphere of data was collected using ω scans with 5 s frame exposures and 0.3° frame widths. Data collection, initial indexing, and cell refinement were handled using APEX II software.⁹ Frame integration, including Lorentz polarization corrections, and final cell parameter calculations were carried out using SAINT+ software.¹⁰ The data were corrected for absorption using the SADABS program.¹¹ The decay of reflection intensity was monitored via the analysis of redundant frames. The structure was solved using direct methods and different Fourier techniques. All hydrogen atom positions were idealized and rode on the atom they were attached to. The final refinement included anisotropic temperature factors on all non-hydrogen atoms. Structure solution, refinement, graphics, and creation of publication materials were performed using SHELXTL.¹² Key crystallographic data are given in Table 1.

Calorimetry of the Dimerization Reaction. A stock solution of 0.52 g of $\text{Mo}(\text{CO})_3(\text{P}^i\text{Pr}_3)_2$ in 11 mL of freshly distilled toluene was prepared in a Schlenk tube under argon inside the glovebox. A 1 mL sample was removed to run a FTIR spectrum of the stock solution, and then 4 mL of the solution was loaded into the mixing cell of the Calvet calorimeter. Recrystallized PhTeTePh (22.8 mg) was added to the solid sample chamber. The calorimeter cell was

(9) APEX II, version 1.08; Bruker AXS, Inc.: Madison, WI, 2004.

(10) SAINT+, version 7.06; Bruker AXS, Inc.: Madison, WI, 2003.

(11) Sheldrick, G. SADABS, version 2.03; University of Göttingen: Göttingen, Germany, 2001.

(12) SHELXTL, version 6.10; Bruker AXS, Inc.: Madison, WI, 2000.

sealed and taken from the glovebox to the calorimeter. After temperature equilibration at 30 °C, the reaction was initiated. Following an initial rapid rise in temperature, the signal did not return to baseline until after more than 4 h in keeping with an initial rapid reaction followed by a slow secondary reaction. Following final equilibration, the cell was taken back into the glovebox and opened under an argon atmosphere, and a FTIR spectrum was run. The only peaks present were those due to [Mo(μ -TePh)(CO)₃(PⁱPr₃)₂] and Mo(CO)₃(PⁱPr₃)₂ as well as a small amount of Mo(CO)₄(PⁱPr₃)₂ which was present in the original stock solution. The remaining solution from the original stock solution was used for a second determination. The measured total enthalpy of reaction, $\Delta H = -24.6 \pm 1.1$ kcal mol⁻¹, is the average of five separate measurements. It was corrected for the endothermic enthalpy of solution of PhTeTePh (+6.2 \pm 0.2 kcal mol⁻¹) to give a total $\Delta H = -30.2 \pm 1.3$ kcal mol⁻¹.

Kinetics Studies of the Dimerization of *Mo(TePh)(CO)₃(PⁱPr₃)₂. In the glovebox, 0.395 g of Mo(CO)₃(PⁱPr₃)₂ was weighed into a Schlenk tube and under an atmosphere of N₂ was dissolved in 40 mL of freshly distilled toluene. The solution was loaded into two 20 mL syringes, taken from the glovebox, loaded into a thermostatted glass reactor, also under N₂ atmosphere, and attached to the flow-through cell of the FTIR microscope by Teflon tubing. Following temperature equilibration at 32.8 °C, a solution of 0.160 g of PhTeTePh in 5 mL of toluene was added to the reactor to generate an in situ solution of *Mo(TePh)(CO)₃(PⁱPr₃)₂. The reactor was covered with aluminum foil to exclude light. The reaction was monitored by periodically withdrawing a fresh 2 mL sample from the thermostatted reactor and rapidly scanning its spectrum. Reaction was studied in the absence and in the presence of added additional PⁱPr₃.

Reaction of *Mo(TePh)(CO)₃(PⁱPr₃)₂ with Py and CO. An in situ solution of *Mo(TePh)(CO)₃(PⁱPr₃)₂ was prepared in a Schlenk tube from 0.05 g of Mo(CO)₃(PⁱPr₃)₂ and 0.021 g of PhTeTePh in 8 mL of toluene. A FTIR spectrum of the green-blue solution taken immediately after the addition of the solvent showed bands at 1973 and 1875 cm⁻¹. To this solution was added 0.5 mL of pyridine which resulted in an instantaneous conversion of the green-blue color of the radical complex to the characteristic red-purple color of Mo(py)(CO)₃(PⁱPr₃)₂. A FTIR spectrum run within a few minutes confirmed quantitative conversion with bands at 1935 and 1817 cm⁻¹.

Exposure of an in situ solution of *Mo(TePh)(CO)₃(PⁱPr₃)₂, prepared as described above, to an atmosphere of CO resulted in the rapid bleaching of all color upon swirling to yield a pale yellow nearly colorless solution of Mo(CO)₄(PⁱPr₃)₂ with ν CO = 1871 cm⁻¹.

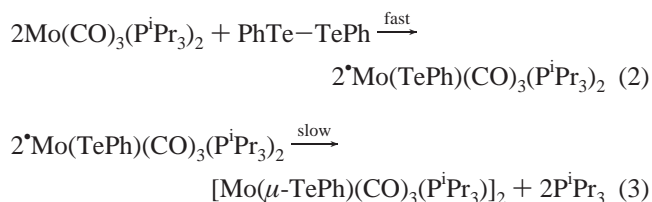
Failure of *Mo(SePh)(CO)₃(PⁱPr₃)₂ To React with Py. An in situ solution of *Mo(SePh)(CO)₃(PⁱPr₃)₂ was prepared in a Schlenk tube from 0.038 g of Mo(CO)₃(PⁱPr₃)₂ and 0.013 g of PhSeSePh in 10 mL of toluene. A FTIR spectrum of the blue solution taken immediately after the addition of the solvent showed bands at 1981 and 1873 cm⁻¹. To this solution was added 0.5 mL of pyridine which resulted in no change in color or FTIR spectrum. Kept under argon atmosphere overnight, the solution retained its blue color overnight, and the FTIR spectrum was essentially unchanged, indicating no reaction.

Kinetics Studies of the Reaction of (*TePh)W(CO)₃(PⁱPr₃)₂ and CO. A solution of *W(TePh)(CO)₃(PⁱPr₃)₂ was prepared in a Schlenk tube from 0.8 g of W(CO)₃(PⁱPr₃)₂ and 0.3 g of PhTeTePh in 40 mL of freshly distilled toluene under argon atmosphere. The solution was loaded into two 20 mL syringes, taken from the glovebox, loaded into a thermostatted glass reactor, also under argon

atmosphere, and attached to the flow-through cell of the FTIR microscope by Teflon tubing. Following temperature equilibration, the atmosphere above the solution was rapidly evacuated and replaced by CO at 1.6 atm of total pressure. (*Note: Carbon monoxide was vented to the hood—caution must be taken in working with CO.*) This purge cycle was repeated twice during which time the reactor was vigorously shaken to increase the rate of gas uptake. During the reaction, the reactor was covered with aluminum foil to exclude light and was vigorously stirred. The reaction was monitored by periodically withdrawing a fresh 2 mL sample from the thermostatted reactor and followed rapidly by an IR scan. The reaction was studied in the absence and in the presence of excess PⁱPr₃.

Results and Discussion

Phosphine Elimination from *Mo(TePh)(CO)₃(PⁱPr₃)₂ Forming [Mo(TePh)(CO)₃(PⁱPr₃)₂]. During an initial calorimetric study⁵ of reactions such as that shown in eq 2, we used the relatively slow technique of Calvet calorimetry to investigate all combinations of the reaction of M(CO)₃(PⁱPr₃)₂ and PhE–EPh (M = Mo, W; E = S, Se, Te). For all combinations except Mo(CO)₃(PⁱPr₃)₂ and PhTe–TePh, an initial rapid exothermic reaction was followed by a smooth return to baseline in the calorimeter signal. For Mo(CO)₃(PⁱPr₃)₂ and PhTe–TePh, however, a return to baseline took several hours, which indicated the occurrence of a slow secondary reaction. Upon opening the calorimeter cell, the bright green color of the (*TePh)Mo(CO)₃(PⁱPr₃)₂ radical had been replaced by a red-brown complex with a different FTIR spectrum. A subsequent independent synthetic study showed that the two-step process occurring in the calorimeter at 30 °C corresponded to the reactions shown in eqs 2 and 3 and that these occurred quantitatively as shown:



The presence of free PⁱPr₃ was detected both by its characteristic unpleasant smell and by its secondary reaction chemistry. Spectroscopic analyses (IR, NMR, MS) as well as elemental analyses of the isolated product all agreed with its formulation as being the diamagnetic bridging dimeric complex shown in eq 3, which would be expected to have a metal–metal bond. Attempts to grow crystals suitable for an X-ray structural analysis of [Mo(TePh)(CO)₃(PⁱPr₃)₂] were unsuccessful. However, the related naphthalene-substituted complex [Mo(Te–naphthyl)(CO)₃(PⁱPr₃)₂] did produce crystals suitable for study, and this structure is shown in Figure 2.

The Mo–Mo distance of 3.2130 Å is observed and is indicative of a Mo–Mo bond which is slightly shorter than that for the Mo(I) dimeric complex [C₅H₅(CO)₃Mo–Mo(CO)₃C₅H₅] with a Mo–Mo vector of 3.235 Å.¹³ The Mo–

(13) Adams, R. D.; Collins, D. M.; Cotton, F. A. *Inorg. Chem.* **1974**, *13*, 1086.

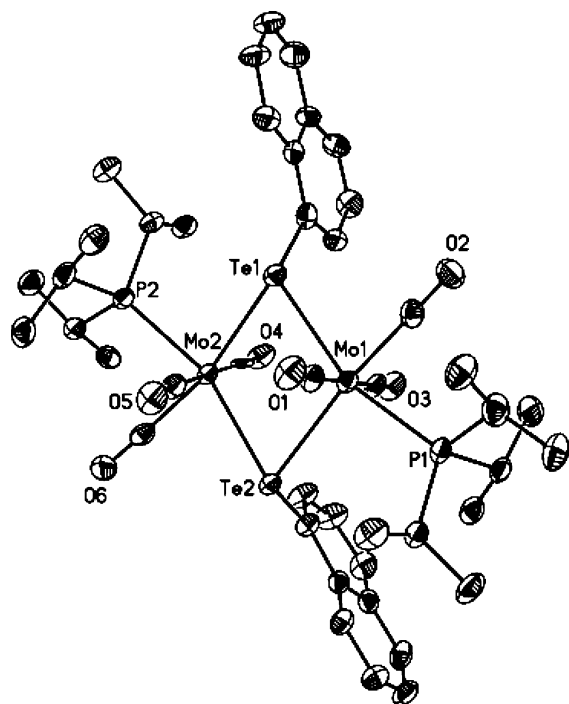


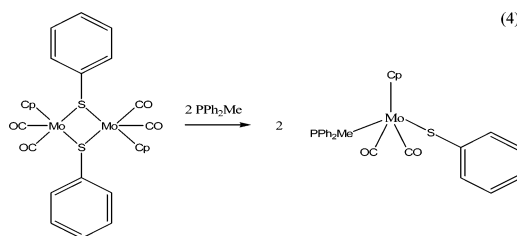
Figure 2. Crystal structure of $[\text{Mo}(\mu\text{-Te-naphthyl})(\text{CO})_3(\text{P}^i\text{Pr}_3)]_2$. Full crystallographic data are available in Supporting Information.

Mo bond for $[\text{Mo}(\mu\text{-Te-naphthyl})(\text{CO})_3(\text{P}^i\text{Pr}_3)]_2$ reported here is longer than that reported earlier for the less sterically crowded complex^{2,3} $[\text{Mo}(\mu\text{-TePh})(\text{CO})_4]_2$ ($\text{Mo-Mo} = 3.114 \text{ \AA}$). It is also of interest that the Mo-Te bond length in $[\text{PhTe-TePh}][\text{Mo}(\text{CO})_5]_2$ (2.779 Å), in which oxidative addition has not occurred, is quite close to that in the complex $[\text{Mo}(\mu\text{-Te-naphthyl})(\text{CO})_3(\text{P}^i\text{Pr}_3)]_2$ (Figure 1, 2.76 Å) and also to that reported for $[\text{Mo}(\mu\text{-TePh})(\text{CO})_4]_2$ (2.746 Å). This indicates that oxidative addition of phenyl ditelluride, at least for these cyclic complexes, does not result in a significant change in the M-TePh bond length.

Thermochemical Estimate of the Mo–Mo Bond Strength in $[\text{Mo}(\mu\text{-TePh})(\text{CO})_3(\text{P}^i\text{Pr}_3)]_2$. Calvet calorimetric measurements over a period of 4 h at 30 °C yielded reproducible results for the sum of reactions 2 and 3: $\Delta H = -30.2 \pm 1.3 \text{ kcal mol}^{-1}$. Deconvolution of the thermogram into a fast first process and a slower secondary process gave a value of $-21.2 \text{ kcal mol}^{-1}$ for the first process (reaction 2) and $-9.0 \text{ kcal mol}^{-1}$ for the slower secondary reaction (reaction 3).¹⁴ The separate measurement of reaction 3 by rapid calorimetry gave an independent value⁵ of $\Delta H = -21.4 \text{ kcal mol}^{-1}$, in good agreement with the value obtained by resolution of the fast and slow response signals in the thermogram.

It is well-known that dimeric bridging chalcogenide complexes can, in some cases, be cleaved by the addition of

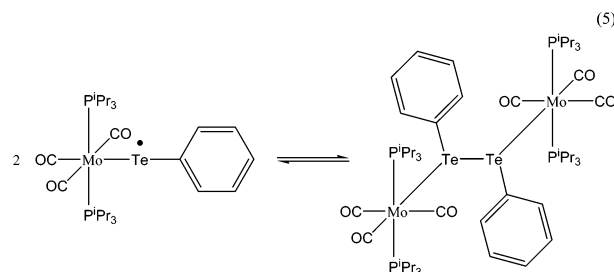
a ligand. For example, we have previously reported¹⁵ the enthalpy of reaction 4:



Attempts to reverse reaction 3 by the addition of phosphine were not successful and indicate that reaction 3 is irreversible under these conditions. That is in keeping with the exothermic nature of reaction 3 as well as the expectation that entropic factors would also favor it because of the release of the 2 mol of phosphine during the reaction.

A plausible reason that reaction 3 cannot be reversed by the addition of phosphine is the presence of the metal–metal bond in the dimeric complex $[\text{Mo}(\mu\text{-TePh})(\text{CO})_3(\text{P}^i\text{Pr}_3)]_2$ which is of the structural type **2C**. It is the absence of the metal–metal bond in the $\text{Mo}(\text{II})$ complex $[\text{Mo}(\mu\text{-SPh})\text{Cp}(\text{CO})_2]_2$ (type **2D**) which allows cleavage of the cluster by phosphine. The difference of $\approx 30 \text{ kcal mol}^{-1}$ between the exothermic ($\Delta H = -21.0 \text{ kcal mol}^{-1}$) reaction 4 and the endothermic ($\Delta H = +9.0 \text{ kcal mol}^{-1}$) value for the reverse of reaction 3 indicates that the value of the Mo-Mo bond in $[\text{Mo}(\mu\text{-TePh})(\text{CO})_3(\text{P}^i\text{Pr}_3)]_2$ is on the order of $\approx 30 \text{ kcal mol}^{-1}$. Considering the rough nature of this approximation, we find that the result appears reasonable on the basis of the reported $\text{Mo}(\text{I})\text{-Mo}(\text{I})$ bond strength in $\text{Cp}(\text{CO})_3\text{Mo-Mo}(\text{CO})_3\text{Cp}$ of $32.5 \text{ kcal mol}^{-1}$.¹⁶

Mechanistic Studies of Dimer Formation by $\cdot\text{Mo}(\text{TePh})(\text{CO})_3(\text{P}^i\text{Pr}_3)_2$. The initial goal of this work was to gain evidence that the formation of the bridging dimeric complexes from the monomeric radicals occurred via the reversible equilibrium shown in eq 5:



This is the first step in the mechanism shown in Figure 1. In view of the established structure of the pentacarbonyl complexes shown in eq 1 and the fact that the lowest enthalpy of the oxidative addition of PhE-EPh ($\text{E} = \text{S, Se, Te}$) to $\text{M}(\text{CO})_3(\text{P}^i\text{Pr}_3)_2$ ($\text{M} = \text{Mo, W}$) occurs for $\text{E} = \text{Te}$ and $\text{M} = \text{Mo}$, reaction 5 is plausible. Nevertheless, attempts to monitor

(14) Deconvolution of the thermogram was accomplished by importing the data for the temperature/time profile of a fast reaction done under identical conditions, normalizing the initial maximum response to scale and using computer subtraction and integration to resolve the fast and slow components as relative fractions of the total heat. Experimental error to this procedure is not assigned since we rely instead on direct measurement by rapid response calorimetry of the fast first reaction. The agreement between the two approaches is good.

(15) Mukerjee, S. L.; Gonzalez, A. A.; Nolan, S. P.; Ju, T. D.; Lang, R. F.; Hoff, C. D. *Inorg. Chim. Acta* **1995**, *240*, 175.

(16) Amer, S.; Kramer, G.; Poe, A. J. *Organomet. Chem.* **1975**, *220*, 75.

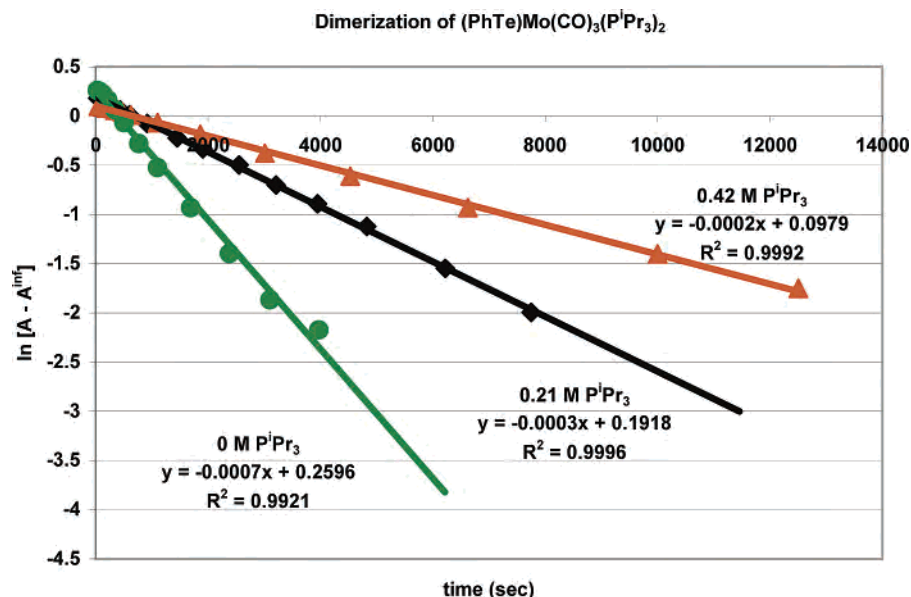


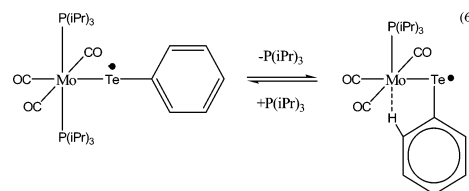
Figure 3. First-order plots of $\ln[A^\infty - A]$ for reaction 5 at different initial phosphine concentrations: green plot initial $[\text{P}^i\text{Pr}_3] = 0 \text{ M}$, black plot initial $[\text{P}^i\text{Pr}_3] = 0.21 \text{ M}$, orange plot initial $[\text{P}^i\text{Pr}_3] = 0.42 \text{ M}$. Reactions in toluene are at 32.8°C under argon atmosphere. (\blacktriangle , $0.42 \text{ M P}^i\text{Pr}_3$; \blacklozenge , $0.21 \text{ M P}^i\text{Pr}_3$; \bullet , $0 \text{ M P}^i\text{Pr}_3$)

the establishment of the equilibrium process in eq 5 by low-temperature FTIR analysis did not show a formation of detectable amounts of a dimeric complex, even at temperatures as low as -80°C .¹⁷

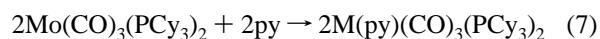
Failure to detect $(\mu\text{-PhTe-TePh})[\text{Mo}(\text{CO})_3(\text{P}^i\text{Pr}_3)_2]_2$ spectroscopically does not obviate its potential role as a key reactive intermediate. Kinetic studies were begun in order to determine the reaction order in $[\text{M}(\text{TePh})(\text{CO})_3(\text{P}^i\text{Pr}_3)_2]$. Reaction mechanisms, beginning with the equilibrium shown in eq 5, would be expected to be second-order in $[\text{M}(\text{TePh})(\text{CO})_3(\text{P}^i\text{Pr}_3)_2]$. In dealing with air-sensitive complexes, it can be difficult at times to distinguish positively between first- and second-order dependence on metal concentration.¹⁸ In addition, during the course of these studies, it was determined that the dimerization of $\text{M}(\text{TePh})(\text{CO})_3(\text{P}^i\text{Pr}_3)_2$ was inhibited by the presence of P^iPr_3 in solution. Since this is released as the dimer is formed, the reaction is expected to be slowed as it proceeds.

In spite of these difficulties, plots of $\ln[\text{M}(\text{TePh})(\text{CO})_3(\text{P}^i\text{Pr}_3)_2]$ versus time were found to provide the best fit to experimental data. Second-order plots of $[\text{M}(\text{TePh})(\text{CO})_3(\text{P}^i\text{Pr}_3)_2]^{-1}$ had poor correlation coefficients. As shown in Figure 3, the reaction rate was found to decrease with added P^iPr_3 . These observations suggest that dimer formation *does not* proceed by reaction 5 or the mechanism in Figure 1. Rate laws with this step initiating the reaction will lead to second-order dependence in metal concentration even if reversible phosphine elimination occurs following this step.

For a reaction first order in metal and inhibited by phosphine, the ligand dissociation shown in eq 6 provides a potential first step consistent with our observations.¹⁹



Ligand Induced Reductive Elimination of PhTeTePh in Reactions of $\text{M}(\text{TePh})(\text{CO})_3(\text{P}^i\text{Pr}_3)_2$ ($\text{M} = \text{Mo}, \text{W}$) with Pyridine and Carbon Monoxide. Data confirming the kinetic role of the equilibrium shown in eq 5 to support the mechanism shown in Figure 1 for dimer formation from the monomeric radical complexes could not be found. This possibility was further probed in reaction with strong ligands for these complexes. The enthalpy of oxidative addition of phenyl ditelluride is sufficiently low⁵ ($\Delta H = -21.4 \text{ kcal mol}^{-1}$) that it is less than the enthalpies of ligand binding of many strong ligands in this system.²⁰ For example, the enthalpy of binding of 2 mol of pyridine, as shown in eq 7, is exothermic by $\approx -34 \text{ kcal mol}^{-1}$.



(17) An initial attempt at detecting this equilibrium in the temperature range -40 to -80°C in toluene appeared to show some spectroscopic changes; however, those results were never reproduced. On four separate attempts, the authors could find no conclusive evidence that the bands assigned to the monomeric radical complex associate in solution at low temperature.

(18) Ju, T. D.; Capps, K. B.; Roper, G. C.; Hoff, C. D. *Inorg. Chim. Acta* **1998**, *270*, 488.

(19) The subsequent steps leading to dimer formation could involve rearrangement of this radical, combination with the starting material, and ultimately production of product. These lead to complex rate laws which would be difficult to prove. The only conclusion that authors can make is that the radical recombination scheme in Figure 1 is not supported by our data, and a mechanism starting with a mononuclear reaction such as that shown in eq 6 mechanism could be supported.

(20) (a) Hoff, C. D. *Prog. Inorg. Chem.* **1992**, *40*, 503. (b) Reaction of $\text{Mo}(\text{P}^i\text{Pr}_3)_2(\text{CO})_3$ with Py is more exothermic by $1-2 \text{ kcal mol}^{-1}$ than the reported data for $\text{Mo}(\text{PCy}_3)_2(\text{CO})_3$ (unpublished results).

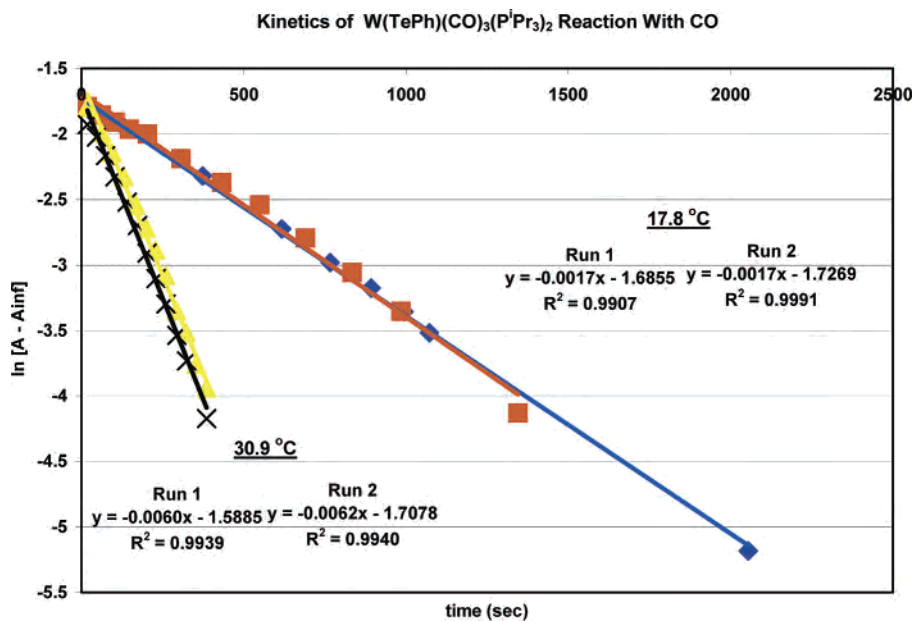
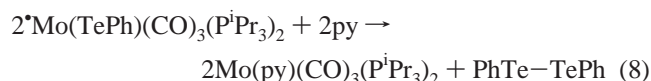


Figure 4. First-order plots of $\ln(A - A_{\infty})$ for the reaction of $W(TePh)(CO)_3(P^iPr_3)_2$ with CO under pseudo-first-order conditions ($P_{CO} = 1.6$ atm) in toluene²⁴ at 17.8 and 30.9 °C. (\blacktriangle , 30.9 °C run 1; \times , 30.9 °C run 2; \blacklozenge , 17.8 °C run 1; \blacksquare , 17.8 °C run 2).

This implies the thermodynamic feasibility of ligand induced reductive elimination as shown in reaction 8 which should be exothermic by ≈ -13 kcal mol⁻¹.

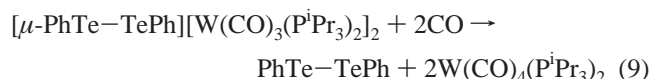


While entropic factors should disfavor reaction 8 (with $T\Delta S \approx 10$ kcal mol⁻¹ at room temperature²¹), the enthalpy of ligand binding is sufficiently exothermic that reaction 8 should occur.

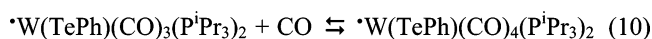
Addition of excess pyridine to green-blue toluene solutions of $W(TePh)(CO)_3(P^iPr_3)_2$ causes a rapid color change to red-purple. Spectroscopic analysis shows quantitative conversion to $Mo(py)(CO)_3(P^iPr_3)_2$. Reaction with pyridine was too rapid to allow its study by conventional kinetics. The corresponding reaction with CO also proceeds quantitatively to produce $Mo(CO)_4(P^iPr_3)_2$. This reaction was also complete within seconds of mixing the reagents. The rapid reaction of $W(TePh)(CO)_3(P^iPr_3)_2$ with pyridine was not observed for $W(SePh)(CO)_3(P^iPr_3)_2$ which showed no detectable reaction with excess pyridine overnight.²²

The reaction of $[W(TePh)(CO)_3(P^iPr_3)_2]$ and CO was slow enough that it could be followed using conventional kinetics techniques. Two reasonable mechanisms can be proposed

for reductive carbonylation. The first would involve the monomer/dimer equilibrium shown in reaction 6. It is well-known that coordinate bonds between $M(CO)_3(P^iPr_3)_2$ ($M = Cr, Mo, W$) and weak donor ligands such as H_2, N_2 , nitrile, and tetrahydrothiophene are rapidly displaced¹ by CO, and it would be expected that displacement of $PhTe-TePh$ would be facile. Thus, one plausible mechanism for reductive carbonylation would be the establishment of the monomer/dimer equilibrium shown in eq 5 followed by a rapid ligand replacement shown in eq 9.



A second plausible mechanism is based on the known rapid ligand substitution reactions of $17e^-$ radical complexes via associative reactions involving $19e^-$ intermediates.²³ In these substitutions, however, it is typically not the radical ligand that is displaced. Nevertheless, a reasonable mechanism for reductive carbonylation based on this premise would be that shown in eq 10:



↓



As shown in Figure 4, kinetic studies of the rate of reaction with CO showed first- and not second-order dependence on $[W(TePh)(CO)_3(P^iPr_3)_2]$ and thus are not in keeping with a mechanism based on reactions 6 and 9 but are more in keeping with a mechanism such as that shown in eq 10 involving associative displacement of a $TePh$ radical. The data in Figure 4 yield a value of $E_a = +17.2$ kcal mol⁻¹ for reaction 10.

(21) This estimate is based on use of the Sackur–Tetrode equation for translational entropy (see Stull, D. R.; Westrum, E. F., Jr.; Sinke, G. C. *The Chemical Thermodynamics of Organic Compounds*; Wiley: New York, 1969. For an approximate application to reactions in solution see: Page, M. I. *Angew. Chem., Int. Ed. Engl.* **1977**, *16*, 449.

(22) It is possible that this is a thermodynamic consequence of the fact that oxidative addition of $PhSeSePh$ is 6.4 kcal mol⁻¹ more exothermic than the addition of $PhTeTePh$.⁵ That would make ligand displacement by pyridine exothermic by only ≈ -6 kcal mol⁻¹ in the case of $[W(SePh)(CO)_3(P^iPr_3)_2]$. The exothermicity of the reaction would not be sufficient to overcome the unfavorable $T\Delta S \approx 10$ kcal mol⁻¹. Kinetic factors cannot, however, be ruled out since it would be expected that there would be more steric congestion in the complexes $[W(EPh)(CO)_3(P^iPr_3)_2]$ as E goes from Te to Se to S.

(23) Basolo, F. *Polyhedron* **1990**, *9*, 1503.

Released $\bullet\text{TePh}$ radicals could either form PhTeTePh by dimerization or react with $\bullet\text{W}(\text{TePh})(\text{CO})_3(\text{P}^i\text{Pr}_3)_2$ to form $\text{W}(\text{PhTe}-\text{TePh})(\text{CO})_3(\text{P}^i\text{Pr}_3)_2$ which would then undergo subsequent rapid ligand substitution as discussed earlier. Displacement of radicals is generally an uphill process since radical species are typically unstable, high-energy species. However, for the $19 e^-$ intermediate complex $\bullet\text{W}(\text{TePh})(\text{CO})_4(\text{P}^i\text{Pr}_3)_2$, the $\text{W}-\text{CO}$ bond²⁵ ($\approx 36 \text{ kcal mol}^{-1}$) is slightly stronger than the $\text{W}-\text{TePh}$ bond⁵ ($\approx 34 \text{ kcal mol}^{-1}$); therefore, displacement of $\bullet\text{TePh}$ is calculated to be thermodynamically allowed.

Conclusion

The principle goal of this work was to gain evidence that there was an equilibrium established in which 2 mol of the $\bullet\text{Mo}(\text{TePh})(\text{CO})_3(\text{P}^i\text{Pr}_3)_2$ radical reformed a $\text{Te}-\text{Te}$ bond to form $[\mu\text{-PhTe}-\text{TePh}][\text{Mo}(\text{CO})_3(\text{P}^i\text{Pr}_3)_2]_2$. Such an equilibrium seems reasonable in view of (i) the known structure of $[\mu\text{-PhTe}-\text{TePh}][\text{M}(\text{CO})_5]_2$ which does not dissociate into radicals, (ii) the known low barriers²⁶ to recombination of chalcogenyl radicals, and (iii) the low enthalpy of oxidative addition of $\text{PhTe}-\text{TePh}$ to $\text{Mo}(\text{CO})_3(\text{P}^i\text{Pr}_3)_2$.

In spite of the reasonable nature of the presumption that the equilibrium in eq 6 should play a role in the chemistry of the $\bullet\text{Mo}(\text{TePh})(\text{CO})_3(\text{P}^i\text{Pr}_3)_2$ radical, *no experimental evidence proving this was found*. Even at low temperatures ($\approx -80 \text{ }^\circ\text{C}$), no spectroscopic evidence for the buildup of a significant concentration of this complex could be found. In addition, the slow conversion of $\bullet\text{Mo}(\text{TePh})(\text{CO})_3(\text{P}^i\text{Pr}_3)_2$ to $[\text{Mo}(\mu\text{-TePh})(\text{CO})_3(\text{P}^i\text{Pr}_3)_2]$ was best fit by a mechanism first order in metal radical complex concentration.

(24) The reactions are pseudo-first-order in CO concentration, not in the usual sense that CO is present in large excess but in the sense that its concentration in solution does not change during the course of the reaction. That is due to the fact that the rate of uptake of CO from the gas phase to solution is rapid compared to the overall rate of reaction, and hence, a CO saturated solution is maintained at a constant [CO] throughout the course of the reaction leading to pseudo-first-order kinetics in [CO].

(25) Fortman, G. C.; Isrow, D.; McDonough, J. E.; Weir, J. J.; Kiss, G.; Kubas, G. J.; Scott, B.; Hoff, C. D. Manuscript in preparation.

Failure to find experimental evidence for the expected monomer/dimer equilibrium does not imply it does not have the potential to be established. The only valid conclusion is that the steady-state equilibrium concentration of the dimer is too low to be detected spectroscopically and that the specific reactions studied had lower energy reaction channels first order in $\bullet\text{Mo}(\text{TePh})(\text{CO})_3(\text{P}^i\text{Pr}_3)_2$ under the conditions studied.²⁷

At this time, the authors are not aware of any documented equilibrium between monomeric complexed alkyl or aryl chalcogenyl radical complexes $\bullet\text{M}(\text{ER})(\text{L})_n$ and their dimeric counterparts $(\text{L}_n\text{M})(\text{R})\text{E}-\text{E}(\text{R})(\text{ML}_n)$ obtained by reforming the $\text{RE}-\text{ER}$ bond. The existence of the stable structures $\bullet\text{-Mo}(\text{TePh})(\text{CO})_3(\text{P}^i\text{Pr}_3)_2$ and $[\mu\text{-PhTe}-\text{TePh}][\text{Mo}(\text{CO})_5]_2$, however, gives confidence to the expectation that fine-tuning of the metal complex and its ancillary substituents should produce a complex in which the bound dichalcogenide dimer and its radical monomer are in closely balanced equilibrium. Additional work on the thermodynamics and kinetics of these and related metal chalcogenyl radical complexes is in progress.

Acknowledgment. Support of this work by the National Science Foundation (C.D.H.) and the Department of Energy, Office of Basic Energy Sciences, Chemical Sciences (G.J.K.), is gratefully acknowledged.

Supporting Information Available: Structural tables and complete crystallographic data for $[\text{Mo}(\text{Te-naphthyl})(\text{CO})_3(\text{P}^i\text{Pr}_3)_2]$. This material is available free of charge via the Internet at <http://pubs.acs.org>.

IC061654X

(26) *S-Centered Radicals*; Alfassi, Z. B., Ed.; Wiley: New York, 1999.

(27) In fact, it is possible that the formation of $[\text{Mo}(\mu\text{-TePh})(\text{CO})_4]_2$ from $[\mu\text{-PhTe}-\text{TePh}][\text{M}(\text{CO})_5]_2$ proceeds through dissociation to radicals or some other first step rather than through a mechanism similar to that shown in Figure 1. In spite of the importance of metal complex activation of the $\text{RE}-\text{ER}$ bond, this remains a challenging mechanistic area even for $\text{E} = \text{O}$ and certainly for the heavier congeners.